

# Dark Matter Remnant Shape after M31-Milky Way Merger

Ethan H. S. Figureido,<sup>1\*</sup>

Submission Date: April 11, 2025

**Key words:** Major Merger – R200 Radius – Hernquist Profile – Dark Matter Halo – Halo Shape – Oblate/Prolate/Triaxial – Isodensity Contours – Galaxy – Galaxy Evolution

## 1 INTRODUCTION

The bulk of matter in the universe exists as **dark matter**: a collisionless particle that doesn't emit radiation and interacts only gravitationally with other matter. Dark matter is structured as an invisible cosmic web that spans the universe. This web stretches across the universe in filaments and sheets. At the intersection of these structures, we find **Dark Matter Halos** (DMHs). DMHs are nodes in the dark matter web where regular matter tends to pool, and this makes them sites of galaxy formation and evolution. When gravity pulls nodes together, the galaxies encompassed within them merge as well, altering the structure of the DMH and the galaxies encompassed within.

We use here the [Willman & Strader \(2012\)](#) definition of a **galaxy**: a gravitationally bound set of stars whose properties cannot be explained by a combination of baryons (non-dark matter matter) and Newton's laws of gravity. **Galaxy evolution** pertains to the processes that change the properties and structures of a galaxy overtime. In modern theories of galaxy evolution, galaxy mergers are an important component and occur when two or more galaxies collide. A merger is considered a **major merger** when the galaxies involved in the collision are of about equal mass. As they are the sites of galaxy evolution, DMH properties are tightly linked to the evolutionary history and properties of galaxies. The structure of DMHs is of particular importance. Understanding how different environments produce different halo structures will provide key insight that we can use to understand a galaxy's merger history ([Drakos et al. 2019](#)). For example, the shape of a halo is connected to the previous major merger, being stretched along the merger axis ([Despali et al. 2016](#)). Understanding what environments different shapes emerge in will help us understand galaxy merger histories and may make them a powerful indicator of a galaxy's merger history.

Modern theories of galaxy evolution have been crafted through galaxy modeling and observation; observation acting to refine the constraints of simulations. Many simulations have been created using different methods and simulating different environments, and it is easy to find a study whose considered simulation favors any of the possible shapes a DMH can have. DMHs take four main **halo shapes**: spherical, **oblate**, **prolate**, and **triaxial**. An oblate spheroid is a sphere squashed along an axis such that two of its radii are equal and larger than the radius along the axis of squashing, giving it a grapefruit shape, and a prolate spheroid is a sphere stretched along an axis such that two radii are equal but smaller than the radius along the axis of stretching, giving it an American football shape. A

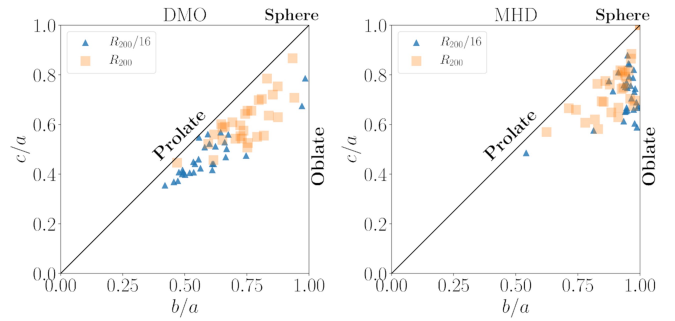


**Figure 1.** Figure 3 from [Prada et al. \(2019\)](#). Plotting the axes ratios for 30 simulated DMHs for dark matter only (DMO, left) and magneto-hydrodynamic (MHD, right) simulations. Triangles indicate data for the inner regions ( $R_{200}/16$  (14kpc)) of the halos. They visualize three main population trends: DMO simulations are rounder in the outer regions than the inner, MHD simulations are rounder in the inner regions than the outer, and MHD halos are rounder than DMO halos, indicating the influence of baryonic matter on the DMH it is encompassed in

triaxial shape is a sphere stretching in two directions such that the radius along each axis is a different length. Using galaxy modeling, we have learned much about these shapes and the environments that favor them. DMHs grow through the accretion of surrounding matter and mergers. In isolation, this growth is anisotropic, favoring triaxial and prolate DMH shapes over spherical or oblate. If we were to consider baryonic processes like black hole feedback, radiative processes, and star formation, we find a smoother, oblate shape. Fig. 1 (Fig.3 from [Prada et al. \(2019\)](#)) illustrates the effects of baryonic processes on halo shape by comparing the axes ratios of halos from magneto-hydrodynamic simulations, which include baryonic effects, and dark matter only simulations which don't. These simulations provide insight into how halos are shaped by the baryonic matter that they encompass.

Much of the uncertainty in this topic stems from the variety of methods and environments used in galaxy simulations, and inadequate resolution. Furthermore, the exact effects of different baryonic processes on DMHs are yet to be adequately determined. The large variety of environments, assumptions, and uncertainties of different simulations has produced evidence favoring each of the four possible halo shapes, as discussed in [Chua et al. \(2019\)](#) and [Prada et al. \(2019\)](#). Many of the open questions surround the reliability of observations and assumptions used to constrain simulations.

\* E-mail: efigureido@gmail.com

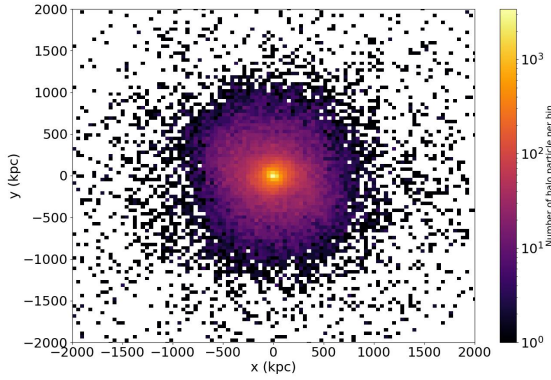


**Figure 2.** Projection of the xy-plane of the merged DMH of the MW and M31 as a 2D number density histogram. It is plotted such that the center of mass is at the origin and the angular momentum vector is aligned in the z-direction. The data is from 8.5 Gyr after the beginning of the simulation and 2.5 Gyr after the merger has completed, corresponding to snapshot 600.

## 2 THIS PROJECT

In this paper, I will study the shape of the merged DMH remnant after the major merger between the Milky Way (MW) and M31, and how the shape evolves overtime.

By analyzing the DMH shape, I aim to replicate the findings of other studies like [Drakos et al. \(2019\)](#), who found the halo shape to stretch along the direction of the merger, and [Prada et al. \(2019\)](#) whose results are displayed in Fig. 1.

DMH shapes are linked to the evolutionary history of galaxies. Studying them can reveal trends that we can apply to other galaxies, unveiling their merger histories.

## 3 METHODS

This study will be conducted using data from the M31-M33-MW merger simulation found in the [van der Marel et al. \(2012\)](#) study. It is an N-body simulation: a dynamical system of particles under the influence of physical forces, in this case gravity. There are three types of particles considered in this simulation: halo, disk, and bulge particles. The disk and bulge particles represent the baryonic matter components of the star, and the halo particles are the dark matter that surrounds them. Particle position, velocity, and mass data are recorded in a series of 800 snapshots which span approximately 11.5 Gyr, capturing the moments before, during, and after the merger.

Using the high resolution simulation data, I will extract the position data of the halo particles for both M31 and the MW after their merger is completed. Using the **R200 radius**, the radius at which the dark matter density is 200 times the critical density of the universe, to define the edge of the halo. To determine the ellipticity of each axis, and thus the shape of the DMH, I will use the position data of the simulated halo particles and plot projections against the xy, xz, and yz-planes, fitting an ellipse to an isodensity contour at the edge of the halo using the photutils python package. Fig. 2 is an example of an xy-plane projection of the merged DMH. This will be done for each snapshot after the merger has been completed. The ellipticity values can be plotted against time, which will allow me to analyze how the shape evolves overtime.

There are few calculations that my code will need to be computed

to retrieve the necessary data. A density profile must be fitted for the combined DMH remnant, so that the edge of the halo can be determined. Using the **Hernquist Profile** from [Hernquist \(1990\)](#), we will determine a density profile, fitting an isodensity contour to determine the halo edge. The Hernquist Profile is defined as equation (1), where  $M_{halo}$  is the total mass of the DMH,  $h_a$  is the scale radius of the Hernquist profile, and  $r$  is the distance from the galactic center. Minimal calculation is needed from here. The virial radius will be found using the Hernquist profile.

$$\rho(r) = \frac{M_{halo}}{2\pi} \frac{h_a}{r(r + h_a)^3} \quad (1)$$

The data will be plotted in many different forms to visualize the dark matter distribution. Projections of the xy, xz, and yz-planes of the DMH will be plotted with an ellipse fit to the isodensity contour that agrees with the virial radius, to visualize the ellipticity of the DMH. The axis ratios will be used to determine its shape. Finding the axis ratios for the DMH for each snapshot after the merger has completed will allow for an analysis of the evolution of the shape. By graphing how the axis ratio changes overtime, we can show how its shape evolves immediately after the merger.

From [Despali et al. \(2016\)](#) a shape elongated along the merger axis is expected. Radiative processes, star formation, and AGN feedback are absent in this simulation. These processes generally smooth the halo to create a more oblate shape, so the simulation is expected to favor a non-oblate shape. Further, because these halos are so large, we expect the growth of the halo to begin with an initially triaxial shape. Combining the above, a triaxial halo with its longest axis in the direction of the merger axis is expected as the merged halo shape.

## 4 RESULTS

By fitting the Hernquist profile of the DMH to its computed mass profile, I found a value of 110 kpc for the scale height of the halo. Using this fitted Hernquist Profile, the R200 radius of the halo was identified at 149 kpc. Isodensity contours were fitted for this radius, defining the edge of the halo in the 3 coordinate planes, as seen in Fig. 4. In this figure, the black ellipse represents the best fit ellipse for a semi-major axis equal to the R200 radius in the xy-projection. The average ellipticity values in each projection over the course of the simulation are:  $\langle \epsilon_{xy} \rangle = 0.09$ ,  $\langle \epsilon_{xz} \rangle = 0.20$ , and  $\langle \epsilon_{yz} \rangle = 0.19$ . These data imply an oblate shape on average after the merger.

Fig. 3 shows results for how ellipticity and axis ratios change overtime. We see high ellipticities and a sharp decreasing trend early after the merger. The plot shows the DMH takes a triaxial shape that slowly decreases in size until snapshot 550 when the xz and yz ellipticities begin to increase, and the xy bounces around the lower values. We see in this data a similar trend between the xy and yz ellipticities in the early snapshots, before the yz breaks away from the xy and follows the xz-projection trend. Its at this point that the halo shape smooths from triaxial to oblate, as the xz and yz ellipticities converge.

## 5 DISCUSSION

The DMH shape is triaxial immediately after the conclusion of the merger. It remains in triaxial form for an extended period, slowly decreasing in size. At snapshot 550, this triaxial shape begins to smooth out, becoming almost perfectly oblate until the end of the simulation. This disagrees with hypothesis, which predicts an initially

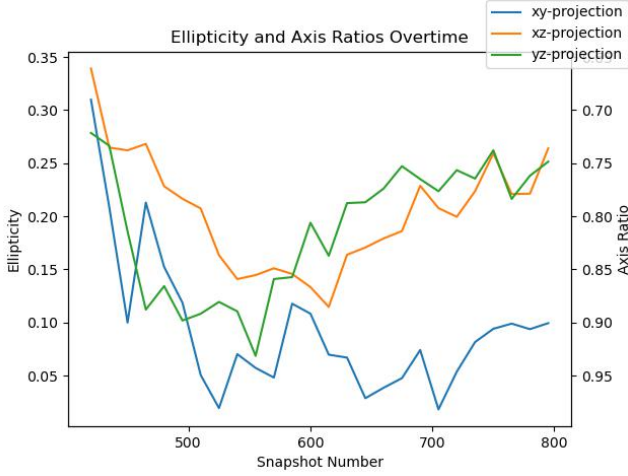


**Figure 3.** A plot of the ellipticity and axis ratios of the best fit isodensity contours for each projection of the DMH overtime. The left axis is the ellipticity, and the right is the axis ratio. The yellow line is the ellipse in the xz-projection, the green is the yz-projection, and the blue is the xy-projection. Time is plotted on the x-axis as snapshot number from snapshot 420 (6 Gyr) to snapshot 795 (11.35 Gyr). This graph shows that the DMH shape is generally triaxial through time after the merger. However, the axes of stretching for this shape shift around snapshot 600 (8.5 Gyr) converging to an oblate shape. Highest ellipticity is found in the earliest snapshots, as matter was still settling after the merger.

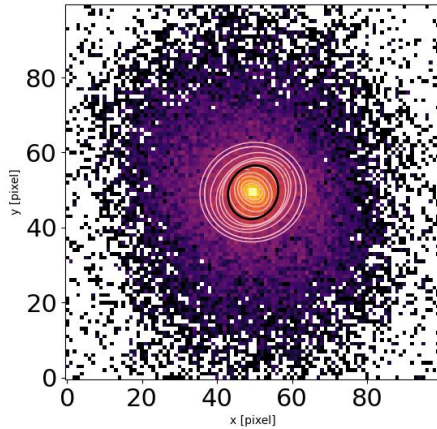


**Figure 4.** A plot of isodensity contours for the xy-projection of the halo at snapshot 600 (8.5 Gyr) on a scale 10 [kpc/pixel]. The pink ellipses represent lines of constant density, for different semi-major axes between 50 and 300 kpc. The black ellipse represents the best fit ellipse with semi-major axis at the edge of the halo as defined by the R200 radius of 149 kpc. For snapshot 600 we have the following ellipticity values:  $\epsilon_{xy} = 0.11$ ,  $\epsilon_{xz} = 0.13$ , and  $\epsilon_{yz} = 0.19$ , which gives the halo a triaxial shape.

triaxial shape that smooths to a prolate one, stretching in the direction of the merger.

These results contradict what is described in [Despali et al. \(2016\)](#) and the trends found in [Prada et al. \(2019\)](#). [Despali et al. \(2016\)](#) describes a halo shape stretched in the direction of the merger, but we our results show an oblate shape, not stretched in one direction,

but squashed in one direction. The data also contradicts what is found in [Prada et al. \(2019\)](#). A simulation lacking MHD processes like this one should favor prolate orientations (Fig. 1). These results are still possible, however. It is possible to attain an oblate halo under these conditions, and the variable results may be due to the high masses of the Mw and M31 haloes. When these two spiral galaxies merge, they become one elliptical galaxy, and this oblate sphere could match the distribution of baryonic matter better than a prolate shape.

A large source of error in this analysis is due to the resolution of the simulation data. Limited by computational power, the low-resolution data was used in favor of the high-resolution, which certainly has affected the data. Further, ellipticity data was computed for every 15 snapshots, which compounds the effect of the low-resolution data.

## REFERENCES

- Chua K. T. E., Pillepich A., Vogelsberger M., Hernquist L., 2019, *Monthly Notices of the Royal Astronomical Society*, 484, 476–493
- Despali G., Giocoli C., Bonamigo M., Limousin M., Tormen G., 2016, *Monthly Notices of the Royal Astronomical Society*, 466, 181–193
- Drakos N. E., Taylor J. E., Berrouet A., Robotham A. S. G., Power C., 2019, *Monthly Notices of the Royal Astronomical Society*, 487, 993–1007
- Hernquist L., 1990, *The Astrophysical Journal*, 356, 5
- Prada J., Forero-Romero J. E., Grand R. J. J., Pakmor R., Springel V., 2019, *Monthly Notices of the Royal Astronomical Society*, 490, 4877–4888
- Willman B., Strader J., 2012, *The Astronomical Journal*, 144, 76
- van der Marel R. P., Besla G., Cox T. J., Sohn S. T., Anderson J., 2012, *The Astrophysical Journal*, 753, 9

This paper has been typeset from a  $\text{\LaTeX}$  file prepared by the author.